

The unsaturated photocurrent controlled by two-dimensional barrier geometry of a single ZnO nanowire Schottky photodiode

Gang Cheng,^{1,2} Zhaohan Li,¹ Shujie Wang,¹ Hechun Gong,¹ Ke Cheng,¹ Xiaohong Jiang,¹ Shaomin Zhou,¹ Zuliang Du,^{1,a)} Tian Cui,² and Guangtian Zou²

¹Key Laboratory for Special Functional Materials of Ministry of Education, Henan University, Kaifeng 475004, People's Republic of China

²National Laboratory of Superhard Materials, Jilin University, Changchun 130012, People's Republic of China

(Received 12 August 2008; accepted 4 September 2008; published online 22 September 2008)

In this letter, the I - V curve of a single ZnO nanowire assembled by dielectrophoresis was measured, which indicated that a back-to-back Schottky barrier structure was formed. Under ultraviolet light illumination, the photocurrent of the ZnO nanowire Schottky photodiode was unsaturated, and its differential conductivity increased with the increase of bias. A two-dimensional Schottky barrier geometry model was introduced to describe the separation of photogenerated electron-hole pairs in the depletion layer, which can well explain the unsaturated photocurrent property. In addition, the corresponding photocurrent equation was obtained, which was in good agreement with the experimental results. © 2008 American Institute of Physics. [DOI: 10.1063/1.2989129]

In recent years, ZnO nanowire (NW) with wide band gap (3.2 eV) has been investigated as photoconductive-type ultraviolet (UV) photodetector.¹⁻⁴ It is widely believed that the photogenerated holes are trapped in the surface states of ZnO NW caused by adsorbed O₂, which decreases the recombination probability of photogenerated electron-hole (e-h) pairs and largely increases the nonequilibrium electron concentration, and then the photocurrent response with ultrahigh on/off ratio from 10⁴ and 10⁶ has been obtained.^{1,2} When the UV illumination is switched off, the chemisorption of O₂ dominates and assists photoconductivity relaxation, which is a slow process from about several seconds to several minutes and largely limits the switching speed.¹⁻⁴ Therefore, it is an important challenge to develop ZnO NW UV photodetector with high speed. Schottky photodiode (SPD) is another commonly used photodetector, which has outstanding advantages of high sensitivity and fast speed due to the high electric field and short transit time in the reverse biased Schottky barrier (SB).⁵⁻⁷ Recently, the photocurrent properties of ZnO NW SPD have been investigated by many groups.^{8,9} For SPD, the photocurrent response is mainly caused by the separation of photogenerated e-h pairs in the depletion layer of SB, therefore, the photocurrent property is closely related to the SB geometry of SPD. However, up to date, there still exists different models to describe the barrier geometry of NW, such as one-dimensional (1D) barrier model¹⁰ and two-dimensional (2D) barrier model.^{11,12} Therefore, it is important to explore the SB geometry of NW and investigate its effect on the photocurrent properties of NW SPD.

In this letter, the photocurrent of a single ZnO NW SPD assembled by dielectrophoresis was investigated, which showed unsaturated photocurrent property. We developed a 2D SB geometry model to describe the separation of photogenerated e-h pairs in the depletion layer, which can well explain the unsaturated photocurrent property.

The ZnO NWs were grown on Si substrates by chemical vapor deposition method, which had been discussed in detail

in our previous report.¹³ In order to measure the electric transport properties, the NWs were first dispersed in ethanol using the sonication method, and then were assembled on a pair of Pt electrodes by dielectrophoresis.^{8,14,15} For dielectrophoresis, an ac voltage with 10 V_{p.p.} (peak to peak) and 50 kHz was applied to the Pt electrode pair. The inset of Fig. 1(a) shows the scanning electron microscopy (SEM) image of a single ZnO NW assembled on a pair of Pt electrodes. The I - V curves of the assembled ZnO NW were measured by semiconductor characteristic measurement system (Keithley 4200 SCS) under room temperature and in air. For photocurrent measurement, a UV light of 350 nm was used.

Figure 1(a) shows the I - V curve of the assembled ZnO NW shown in the inset of Fig. 1(a) in dark, which exhibits nonlinear and asymmetric behavior. Figure 1(b) shows the plot of the I - V curve in log scale in the range from about 2.5 to 5.5 V, which shows linear behavior. According to the detailed discussion by Zhang *et al.*,¹⁰ this linear behavior indicates that the ZnO NW makes two SB contacts with the two Pt electrodes, a back-to-back SB structure is formed, and the current is dominated by the tunneling current of the reverse biased SB, which follows the expression^{10,16}

$$\ln I = \ln(SJ_s) + V \left(\frac{q}{kT} - \frac{1}{E_0} \right), \quad (1)$$

where, S is the contact area of SB, J_s is the reverse saturation current density, k is the Boltzmann constant, T is the absolute

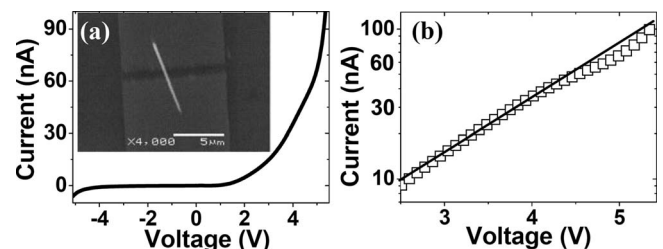


FIG. 1. (a) The typical I - V curve of single ZnO NW between two Pt electrodes. The inset is the SEM image of the measured ZnO NW assembled on the Pt electrodes. (b) The plot of the I - V curve in log scale (hollow square), and its fitted line (solid line).

^{a)} Author to whom correspondence should be addressed. Electronic mail: zld@henu.edu.cn.

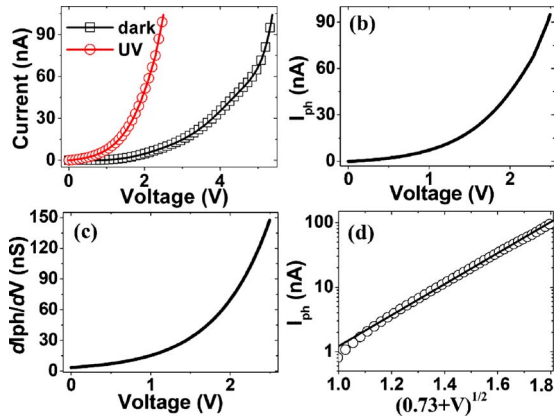


FIG. 2. (Color online) (a) The typical I - V curve of the ZnO NW measured in dark (hollow square) and under illumination (hollow circle). (b) and (c) are the plots of I_{ph} and its differential conductivity with bias, respectively. (d) The plot of I_{ph} with $(\phi_{bi} + V)^{1/2}$ using $\phi_{bi} = 0.73$ eV in log scale (hollow circle), and its fitted line (solid line).

temperature, q is the magnitude of electronic charge, V is the applied reverse bias, and E_0 is a parameter that depends on the carrier density. From the slope of the fitted line in Fig. 1(b), E_0 is obtained as 25.8 mV. According to the relation between E_0 and donor concentration N_D discussed in detail in Refs. 10 and 16, N_D is obtained as 2.95×10^{17} cm $^{-3}$.

According to the previous reports,^{8,15} the asymmetric transport behavior in Fig. 1(a) is related to the dielectrophoresis process. Lao *et al.*¹⁵ suggested that in the dielectrophoresis process, the contact touched first has firmer contact property than that touched later. In the back-to-back SB structure, the positive and negative current are dominated by two different SBs, respectively.^{10,17} As shown in Fig. 1(a), the positive current is much larger than negative current, and the current ratio is about 38.6 at ± 4 V, which indicates that the positive current is dominated by the first touched contact with better contact performance. Therefore, we mainly focus on the positive current in the following photocurrent discussions.

Figure 2(a) shows the I - V curves of the ZnO NW shown in the inset of Fig. 1(a) in dark and under UV illumination with positive bias. Under illumination, the current remarkably increases with current ratio about 10.4 at +2 V, and the curve is still nonlinear. According to the voltage distribution property of the back-to-back SB structure,^{10,17} the nonlinear curve property indicates that the total applied voltage is mainly dropped across the reverse biased SB, and the current is dominated by this SB but not the NW. While for the photoconductive-type photodetector and under illumination condition, two Ohmic contacts are formed in the two ends of the NW, the total applied voltage is mainly dropped across the NW, and the photocurrent response is due to the increase of carrier concentration of NW itself, which generally shows linear curve property.¹⁻⁴ Therefore, the nonlinear I - V curve under illumination shown in Fig. 2(a) represents the photocurrent response of the reverse biased SB but not the NW, and a NW SPD is formed.

Figures 2(b) and 2(c) show the plot of photocurrent I_{ph} [calculated as the difference value between the current under UV light and in dark from the data in Fig. 2(a)] and its differential conductivity with bias, respectively. It is clear that I_{ph} is unsaturated, and its differential conductivity increases with the increase in bias. However, it is well known

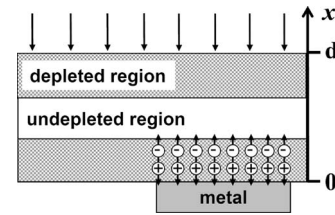


FIG. 3. The band structure diagram of the 2D SB geometry model for ZnO NW SPD.

that the photocurrent of traditional 2D planar SPD is saturated, and its differential conductivity decreases with the increase in reverse bias. This saturated photocurrent property is related to its SB geometry.^{18,19} For planar SPD, the barrier width increases with the increase in reverse bias, while the light intensity and the corresponding photogenerated e-h pairs concentration in the depletion layer decrease exponentially with the increase in barrier width, which causes the differential conductivity decrease with the increase in reverse bias. When the barrier width reaches a critical value (about three absorption depths), the differential conductivity almost decreases to zero, and the photocurrent reaches a saturation value. From above discussions, we can see that the unsaturated photocurrent property of ZnO NW SPD is controlled by its unique SB geometry, which is different with that of planar SPD.

For semiconductor NWs, 1D barrier geometry model is generally used,¹⁰ in which the effect of diameter size of NW is neglected, and the barrier width increases along the long-axis direction of NW with the increase in reverse bias. Recently, the effect of diameter on the photocurrent property of GaN NW photoconductive-type photodetector has been investigated, and a 2D barrier geometry model has been introduced to describe the band bending along the radial direction (perpendicular to the long axis) of NW caused by surface states.^{11,12} Considering the diameter of ZnO NW in this work is about 260 nm, which cannot be neglected, we develop a 2D SB geometry model to describe the ZnO NW SPD. Figure 3 shows the band structure diagram of the 2D SB geometry model, in which the band bending is along the x axis (the radial direction of NW). With the increase in reverse bias, the barrier width of the depletion layer in the contact region increases along the x axis. According to the current image investigation of a single CuO NW in our previous report,¹⁷ the electrons first transfer from the metal into the undepleted region along the x axis, and then transfer along the long axis of NW in the undepleted region.

As shown in Fig. 3, the photogenerated e-h pairs in the depletion layer in the contact region can be effectively separated by the built-in electric field, and then transfer along the x axis, which is the major photocurrent response mechanism for SPD. In addition, some photogenerated e-h pairs in the undepleted region can diffuse into the depletion layer, which can also contribute to the photocurrent. While due to the absence of separation electric field, the separation efficiency for the photogenerated e-h pairs in the undepleted region is much lower than that in the depletion region. Especially, for direct band gap ZnO, the high fluorescence recombination probability further decreases the separation efficiency for the photogenerated e-h pairs in the undepleted region. Therefore, as a proper approximation, we mainly focus on the contribution of the photogenerated e-h pairs in the depletion region,

and neglect that in the undepleted region in the following discussions. In the 2D SB geometry model, since the illumination direction is opposite to the x axis, light intensity in the depletion layer in contact region increases exponentially with the increase in x . Therefore, the concentration of the photo-generated e-h pairs increases exponentially with the increase in bias and barrier width, which determines that the differential conductivity increases with the increase in bias and the photocurrent is unsaturated. Therefore, the 2D SB geometry model can well explain the unsaturated photocurrent property of the ZnO NW SPD.

In the 2D SB geometry model, it is required that the NW is not completely depleted, i.e., $W(0)+W(V)<d$. Here, $W(0)$ is the barrier width at zero bias, $W(V)$ is the barrier width with the bias of V , and d is the diameter of NW (about 260 nm). The barrier width W follows the equation¹⁶

$$W = \sqrt{\frac{2\varepsilon_s(\varphi_{bi} + V)}{qN_D}}, \quad (2)$$

where, φ_{bi} is the barrier height at zero bias, and ε_s is the permittivity of semiconductor. According to Eq. (2), and using $\varepsilon_s=7.9\varepsilon_0$, $N_D=2.95 \times 10^{17} \text{ cm}^{-3}$ (calculated above), and $\varphi_{bi}=0.73 \text{ eV}$ (Ref. 20) (a common barrier height for ZnO SB), it is obtained that the $W(0)=46.5 \text{ nm}$ and $W(2.5)=97.8 \text{ nm}$. Therefore, in the photocurrent measurement bias range in Fig. 2(a) (from 0 to 2.5 V), $W(0)+W(V)<d$ can be well satisfied.

In order to further investigate the relation between SB geometry and the photocurrent property of ZnO NW SPD, the photocurrent equation under the 2D SB geometry is needed. The photocurrent of SPD is generally described by the separation of photogenerated e-h pairs in depletion layer of the reverse biased SB, which can be expressed as^{18,19}

$$I_{ph} = -qS\eta \int_0^W f(x)dx. \quad (3)$$

Here, η is the absorption quantum efficiency (the number of generated e-h pairs per photon), x axis is the direction of band bending, and $f(x)$ is the light intensity distribution function in depletion layer (light intensity denotes the photon number per unit time per unit volume). As discussed above, in the 2D SB geometry model, light intensity increases exponentially with the increase in x , which can be expressed as $f(x)=Fae^{-\alpha(d-x)}$. Here F is the flux density of phonons and α is the absorption coefficient for the photon. Therefore, according to Eqs. (2) and (3), the photocurrent equation is obtained as

$$I_{ph} = Ae^{-\alpha d}(e^{\alpha W} - 1) = Ae^{-\alpha d}(e^{B\sqrt{\varphi_{bi}+V}} - 1), \quad (4)$$

where $A=-qS\eta F$ and $B=\alpha\sqrt{2\varepsilon_s/qN_D}$. Using $\alpha=3.17 \times 10^5 \text{ cm}^{-1}$ (Ref. 21) and the barrier width values calculated above, it is obtained that $e^{\alpha W}$ increases from 4.4 to 22.2 with the bias increasing from 0 to 2.5 V, which indicates $e^{\alpha W} \gg 1$ can be approximately satisfied, and then Eq. (4) can be simplified to $\ln(I_{ph}) \propto (\varphi_{bi}+V)^{1/2}$. Figure 1(d) shows the plot of I_{ph} with $(\varphi_{bi}+V)^{1/2}$ using $\varphi_{bi}=0.73 \text{ eV}$ in log scale, which clearly exhibits linear property. This result indicates that the photocurrent equation of ZnO NW SPD obtained using the 2D SB geometry is in good agreement with the experiment results in this work.

In the 1D SB model for NWs,¹⁰ the light intensity is perpendicular to the band bending direction (the long axis) of NW, and then the light intensity is a constant along the band bending direction. The photocurrent equation using the 1D SB model (can be obtained easily and not shown here) indicates that the differential conductivity decreases with the increase in bias, which cannot explain the unsaturated photocurrent property in this work. In addition, when $W(0)+W(V) \geq d$, the contact region of the NW will be completely depleted, and the relation between the SB geometry and the photocurrent property in this case needs further investigations.

In conclusion, the photocurrent of the ZnO NW SPD assembled by dielectrophoresis was unsaturated. The 2D SB geometry model was introduced to describe the separation of photogenerated e-h pairs in the depletion layer, which can well explain the unsaturated photocurrent property. In addition, the corresponding photocurrent equation was obtained, which can be simplified to $\ln(I_{ph}) \propto (\varphi_{bi}+V)^{1/2}$ and was in good agreement with the experimental results.

This work was supported by the National Natural Science Foundation of China (Grant Nos. 90306010 and 10874040), the Program for New Century Excellent Talents in University of China (Grant No. NCET-04-0653), and the National Basic Research "973" Program of China (Grant No. 2007CB616911). G. Cheng and Z. H. Li contributed equally to this paper.

- ¹H. Kind, H. Q. Yan, B. Messer, M. Law, and P. D. Yang, *Adv. Mater. (Weinheim, Ger.)* **14**, 158 (2002).
- ²C. Soci, A. Zhang, B. Xiang, S. A. Dayeh, D. P. R. Aplin, J. Park, X. Y. Bao, Y. H. Lo, and D. Wang, *Nano Lett.* **7**, 1003 (2007).
- ³Q. H. Li, Q. Wan, Y. X. Liang, and T. H. Wang, *Appl. Phys. Lett.* **84**, 4556 (2004).
- ⁴Z. Y. Fan, P. C. Chang, J. G. Lu, E. C. Walter, R. M. Penner, C. H. Lin, and H. P. Lee, *Appl. Phys. Lett.* **85**, 6128 (2004).
- ⁵S. Alexandrou, C. C. Wang, T. Y. Hsiang, M. Y. Liu, and S. Y. Chou, *Appl. Phys. Lett.* **62**, 2507 (1993).
- ⁶M. Gökkavas, S. Butun, H. B. Yu, T. Tut, B. Butun, and E. Ozbay, *Appl. Phys. Lett.* **89**, 143503 (2006).
- ⁷E. Monroy, F. Omnes, and F. Calle, *Semicond. Sci. Technol.* **18**, R33 (2003).
- ⁸O. Harnack, C. Pacholski, H. Weller, A. Yasuda, and J. M. Wessels, *Nano Lett.* **3**, 1097 (2003).
- ⁹K. Cheng, G. Cheng, S. J. Wang, L. S. Li, S. X. Dai, X. T. Zhang, B. S. Zou, and Z. L. Du, *New J. Phys.* **9**, 214 (2007).
- ¹⁰Z. Y. Zhang, C. H. Jin, X. L. Liang, Q. Chen, and L. M. Peng, *Appl. Phys. Lett.* **88**, 073102 (2006).
- ¹¹L. Polenta, M. Rossi, A. Cavallini, R. Calarco, M. Marso, R. Meijers, T. Richter, T. Stoica, and H. Lüth, *ACS Nano* **2**, 287 (2008).
- ¹²R. Calarco, M. Marso, T. Richter, A. I. Aykanat, R. Meijers, A. V. Hart, T. Stoica, and H. Lüth, *Nano Lett.* **5**, 981 (2005).
- ¹³S. M. Zhou, H. C. Gong, B. Zhang, Z. L. Du, X. T. Zhang, and S. X. Wu, *Nanotechnology* **19**, 175303 (2008).
- ¹⁴P. A. Smith, C. D. Nordquist, T. N. Jackson, T. S. Mayer, B. R. Martin, J. Mbindyo, and T. E. Mallouk, *Appl. Phys. Lett.* **77**, 1399 (2000).
- ¹⁵C. S. Lao, J. Liu, P. X. Gao, L. Y. Zhang, D. Davidovic, R. Tummala, and Z. L. Wang, *Nano Lett.* **6**, 263 (2006).
- ¹⁶E. H. Rhoderick and R. H. Williams, *Metal-Semiconductor Contact* (Clarendon, Oxford, 1988).
- ¹⁷G. Cheng, S. J. Wang, K. Cheng, X. H. Jiang, L. X. Wang, L. S. Li, Z. L. Du, and G. T. Zou, *Appl. Phys. Lett.* **92**, 223116 (2008).
- ¹⁸A. J. Tuzzolino, E. L. Hubbard, M. A. Perking, and C. Y. Fan, *J. Appl. Phys.* **33**, 148 (1962).
- ¹⁹W. W. Gärtner, *Phys. Rev.* **116**, 84 (1959).
- ²⁰M. S. Oh, D. K. Hwang, J. H. Lim, Y. S. Choi, and S. J. Park, *Appl. Phys. Lett.* **91**, 042109 (2007).
- ²¹E. M. Wong and P. C. Searson, *Chem. Mater.* **11**, 1959 (1999).